Spreading of correlations in a quenched repulsive and attractive one-dimensional integrable system

Spreading of correlations in a quenched repulsive and attractive one-dimensional integrable system

L. Barbiero[1,2] and L. Dell'Anna[2]

[1]*CNR-IOM DEMOCRITOS Simulation Center and SISSA, Via Bonomea 265, I-34136 Trieste, Italy*

[2]*Dipartimento di Fisica e Astronomia "Galileo Galilei", Università di Padova, 35131 Padova, Italy*

(Received 2 October 2016; revised manuscript received 15 May 2017; published 8 August 2017)

We study the real-time evolution of the correlation functions in a globally quenched interacting one-dimensional lattice system by means of time-adaptive density matrix renormalization group. We find a clear light-cone behavior quenching the repulsive interaction from the gapped density wave regime. The spreading velocity increases with the final values of the interaction and then saturates at a certain finite value. In the case of a Luttinger liquid phase as the initial state, for strong repulsive interaction quenches, a more complex dynamics occurs as a result of bound state formations. From the other side in the attractive regime, depending on where connected correlation functions are measured, one can observe a delay in the starting time evolution and a coexistence of ballistic and localized signals.

DOI: 10.1103/PhysRevB.96.064303

I. INTRODUCTION

A clear understanding of out-of-equilibrium isolated quantum systems is one of the most challenging tasks in quantum physics [1]. In this context a lot of effort has been devoted towards the comprehension of thermalization processes [2,3], the role of conserved quantities [4,5], entanglement dynamics [6–8], and many-body localization [9,10]. A further key point is represented by the typical light-cone shape exhibited by one- and two-point correlation functions once a sudden quench is applied [11–16]. It has been shown [17] that in critical theories the maximum velocity of the spreading of correlations is given by twice the group velocity defined in the final gapless system. Actually the existence of a maximal velocity [18–20], known as the Lieb-Robinson bound, has been shown to exist theoretically in several locally interacting many-body systems. This is due to the short-range interactions which may reduce the propagation of information making its spreading velocity finite. Moreover light-cone propagation of correlations is expected when starting from a nondegenerate initial state that shows an exponential cluster decomposition property [21–23], which is indeed generally valid for local Hamiltonians. The light-cone propagation can be absent in the presence of long-range interaction [24–26] or for some local-spin models [27,28]. Nowadays, thanks to the impressive achievements in the field of ultracold systems [29], the aforementioned results have been tested by means of cold bosons [30,31] and trapped ions [32,33].

Motivated by this intensive work activity in this paper we provide a time-dependent density matrix renormalization group (t-DMRG) [34] analysis of the correlation spreading once a sudden global quench is applied in a system of interacting hard-core bosons equivalent to the spin-1/2 *XXZ* chain. More precisely, in the first section we consider the case when the interaction is repulsive and we show how much the Bethe ansatz approach is able to properly capture the velocity of the excitation propagation. In particular, we will compare the numerical results with the sound velocity of the ground state, obtained by the Bethe ansatz approach. A better comparison should be obtained considering the velocity of excitations above the stationary state at time $t \to \infty$ [15]. A further crucial point is given by the initial particle density distribution. Indeed, when we quench the interaction from a weak to a strong value, many-body bound states can give rise to a multisignal propagation. The role of bound states in quench dynamics has been explored only for certain initial configurations [35], while here we present results for a highly entangled initial state, namely a Luttinger liquid regime. In the attractive-interaction regime, instead, starting from a phase-separated state, it is possible to get two signals, a localized and a ballistic one, similarly to what has been recently found in the Ising spin chain with transverse and longitudinal magnetic field [28]. A crucial role is played by the position at which the correlation function is pinned. Indeed if one of the positions of the two-point correlation functions is taken well inside the occupied bulk, one has to wait a certain time before observing the quantum effect of the correlation spreading.

II. MODEL

The system we consider is composed by N hard-core bosons loaded in L sites of a one-dimensional lattice at half filling $\bar{n} = N/L = 1/2$,

$$H = -J \sum_i (c_i^\dagger c_{i+1} + c_{i+1}^\dagger c_i) + V \sum_i n_i n_{i+1}, \qquad (1)$$

where J is the tunneling amplitude fixing our energy and time scales (where $\hbar = 1$), V is the nearest-neighbor (NN) interaction, while $c_i^\dagger$ (c_i) is the creation (annihilation) operator of a particle in the i site of the lattice. Notice that at half filling, i.e., $\bar{n} = 1/2$, the Hamiltonian (1) turns out to be exactly mapped to (i) the XXZ spin-1/2 model, by performing the Holstein-Primakoff transformation, and (ii) the analogous model with spinless fermions, through a Jordan-Wigner transformation. Remarkably the physics of the model Eq. (1) can be basically studied in the experiments by using dipolar fermions/hard-core bosons [36,37], bosonic mixture [38], and photons [39]. A further key feature of Eq. (1) is given by its integrability [40] which allows one to extract many fundamental properties. In particular it is well known that the phase diagram consists of three different phases: one of them being a gapless Luttinger liquid (LL) in the region $-2 < V < 2$ and two degenerate gapped regimes. The gap appears both for $V < -2$, giving

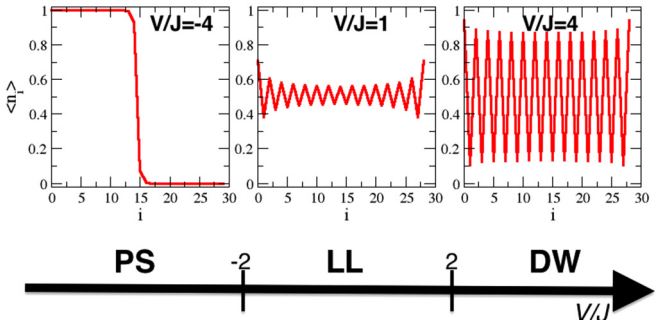

FIG. 1. DMRG density profiles $\langle n_i \rangle$ for the three different regimes for system with $N = 15$ bosons and $L = 30$ sites. The degeneracy of the density wave (DW) is removed by considering $L = 29$ sites, while the degeneracy of the phase separation state (PS) is broken by applying two chemical potentials $\mu/J = 0.001$ with opposite sign at the lattice edges. The simulations are performed by keeping up to 512 DMRG states and 5 finite-size sweeps.

rise to a phase-separated (PS) state with empty and occupied sites totally demixed in two different regions, and for $V > 2$, where a density wave (DW) modulation is present. Notice that the two previous regimes are usually identified in spin language as ferro- and antiferromagnetic regimes.

The relative density profiles $\langle n_i \rangle$, obtained via static DMRG calculations [41] for the three different phases, are shown in Fig. 1. Here we break the ground state degeneracy of the DW and PS phases by respectively considering an odd number of sites and by adding very small antiparallel chemical potentials at the lattice edges. Indeed in the first scenario the choice $N = (L + 1)/2$, with L odd, automatically removes the degeneracy of the ground state but the phase diagram remains unchanged; from the other side, adding two small magnetic fields in the first and last lattice sites favors the clustering of particles in one edge of the system. As shown in [21–23] degeneracy breaking is a crucial ingredient for observing conelike propagation. Indeed for degenerate ground states the cluster decomposition property cannot be defined and consequently the Lieb-Robinson bound velocity is not expected. The weak density modulation appearing in the LL regime is nothing but the well-known phenomenon of the Friedel oscillations [42]. Here the crucial feature, as will be clear in the next part, is that the wave function of any single particle is sufficiently delocalized to allow to two particles to lie in NN sites. This is an obvious difference with respect to the DW regime where the strong repulsive V makes energetically very costly NN occupancies. From the other side PS allows NN occupations due to obvious energetic reasons but the single-particle wave function is localized. For this reason it is important to understand how a certain initial density distribution affects both the spreading of the correlation and its velocity once a sudden quench in the interaction V is applied. In all our simulations we obtain the ground state (GS) relative to a certain V_i and we let the system evolve in time t once the interaction is suddenly brought to a value V_f. We then monitor the relative spreading of the connected density-density correlation function

$$C_{ij}(t) = \langle n_i(t) n_j(t) \rangle - \langle n_i(t) \rangle \langle n_j(t) \rangle. \quad (2)$$

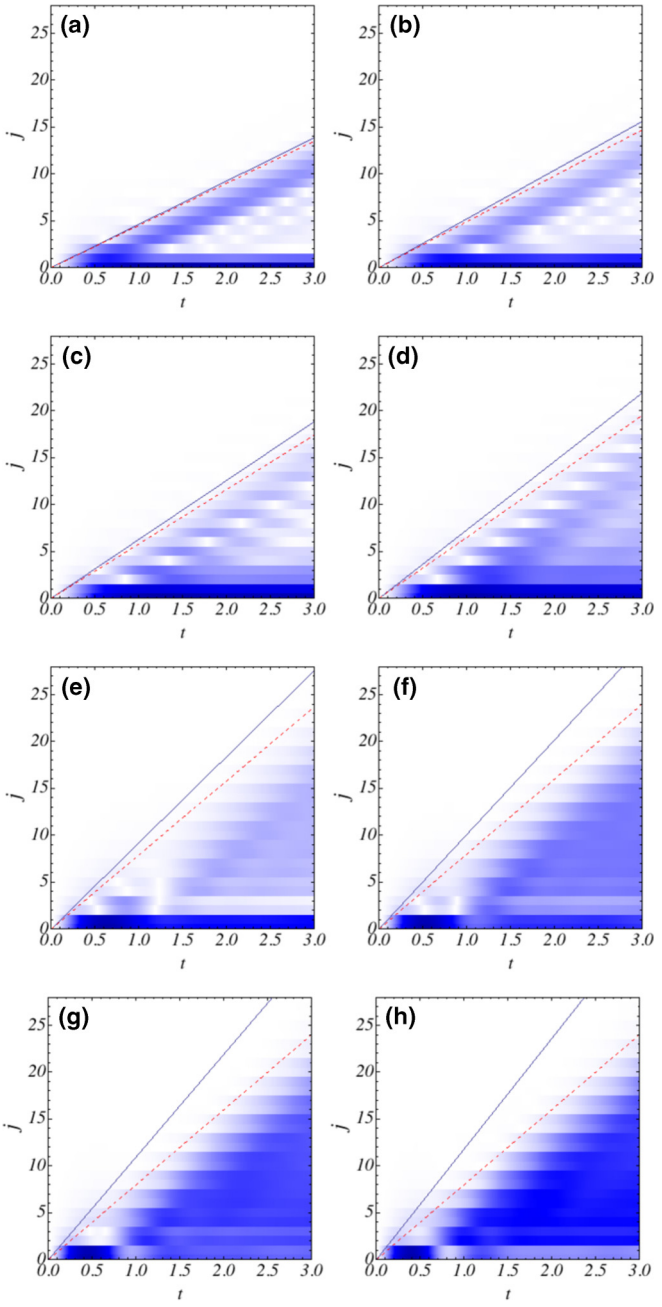

FIG. 2. t-DMRG results of $\Delta C_{ij} = |C_{ij}(t) - C_{ij}(0)|$ for $V_i = 4$ and (a) $V_f = 0.5$, (b) $V_f = 1$, (c) $V_f = 2$, (d) $V_f = 3$, (e) $V_f = 5$, (f) $V_f = 6$, (g) $V_f = 7$, (h) $V_f = 8$. The length of the chain is $L = 29$ and $N = 15$. Both t and the V's are in units of J. The slopes of the solid lines are the velocities v_{BA}, given by Eq. (3), while those of the dashed red lines are the measured velocities reported in Fig. 3, above which the signals are exponentially small. The static simulations for the ground state are performed by keeping up to 512 DMRG states and 5 finite-size sweeps and the dynamics is obtained by using a time step $\delta = 0.01$ and 250 DMRG states.

III. REPULSIVE REGIME

As a first step we investigate the case of a V_i supporting a DW regime. In Fig. 2 we plot $\Delta C_{ij} = |C_{ij}(t) - C_{ij}(0)|$ as a function of t and j, at fixed $i = 0$ (first site of the lattice),

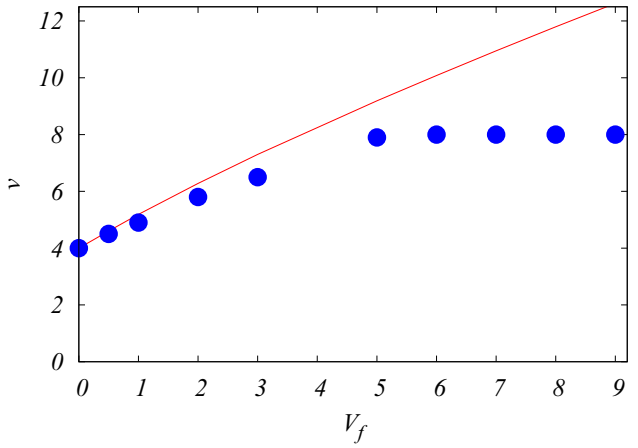

FIG. 3. Spreading velocities for quenches from the initial value $V_i = 4$ to different final values of V_f. The dots are the measured velocities from t-DMRG as in Fig. 2, while the solid red line shows the velocities v_{BA} from the Bethe ansatz approach, given by Eq. (3).

for $V_i = 4$ and several values of V_f, both in the LL and DW phase.

For V_f within the gapless regime, the exact spectrum from the Bethe ansatz approach is available [43], which allows us to predict the spreading velocity v in a gapless phase, which is $v \simeq v_{BA}$, with

$$v_{BA} = 2\pi J \frac{\sqrt{1-(V_f/2J)^2}}{\arccos(V_f/2J)}, \tag{3}$$

twice the sound velocity.

As clearly visible, our numerical results in Fig. 2 are in very good agreement with the analytical solution, for V_f in the LL regime. Furthermore, as already shown in [13], for V_f not too strong, but already able to capture the DW behavior, the Bethe ansatz velocity, extended to $V_f > 2$, is still able to give a description of the spreading velocities. From the other side once V_f exceeds a critical value, the velocity v of the fastest signal seems to saturate to a constant value. In particular, as visible in Figs. 2 and 3, for $V_f \gtrsim 5$ the velocity saturates at the value $v \sim 8$, in agreement with the results reported in [13] for a different value of V_i. As we checked, the aforementioned feature remains valid also for different values of V_i, confirming the belief that the spreading velocity depends mainly on the final interaction strength governing the dynamics. Of course extracting the exact velocity v is not possible within our approach so we can only infer the correctness of the just mentioned results. However a key point to be noticed here is that only one clear and strong single signal is present in the dynamics. The situation becomes rather different once interaction quenches are performed starting from a LL ground state. Several results showing quenches within this regions are present, see [44] and references therein, but the case of strong V_f has not been investigated. As previously mentioned in the gapless regime the density distribution is weakly modulated but the wave functions are rather delocalized thus allowing NN occupancies. As clearly visible in Fig. 4, this aspect has huge consequences in excitation propagation. More precisely in Fig. 4 we start with a LL configuration obtained by getting the ground state for $V_i = 1$ and we let the system

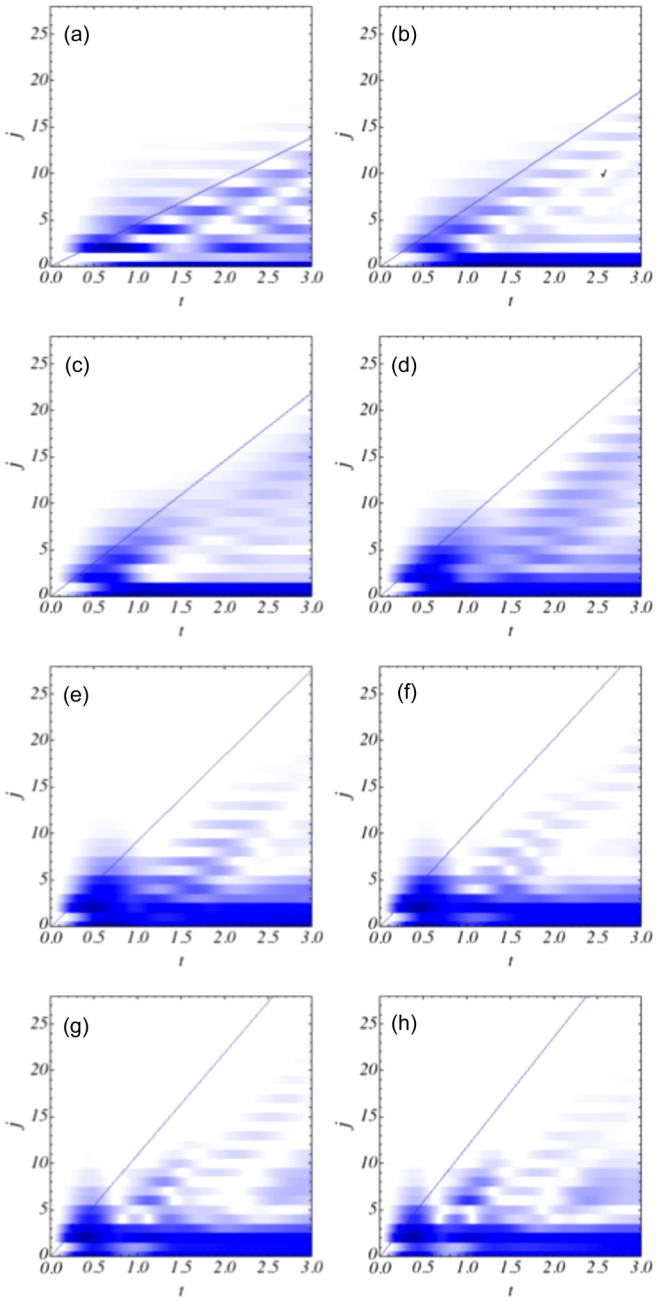

FIG. 4. t-DMRG results of $\Delta C_{ij} = |C_{ij}(t) - C_{ij}(0)|$ for $V_i = 1$ and (a) $V_f = 0.5$, (b) $V_f = 2$, (c) $V_f = 3$, (d) $V_f = 4$, (e) $V_f = 5$, (f) $V_f = 6$, (g) $V_f = 7$, (h) $V_f = 8$. The length of the chain is $L = 30$ and $N = 15$. Both t and the V's are in units of J. The slopes of the solid lines are the velocities v_{BA}, given by Eq. (3). The static simulations for the ground state are performed by keeping up to 512 DMRG states and 5 finite-size sweeps and the dynamics is obtained by using a time step $\delta = 0.01$ and 250 DMRG states.

evolve with different V_f. Clearly when V_f is weak a clear single-signal propagation is visible, resembling the $V_i = 4$ case, but once V_f becomes stronger a multisignal propagation appears. Moreover it is possible to notice that the bigger is V_f the bigger the number of signals contributing to the dynamics is. This effect can be basically explained by starting with a two-particle description, looking at the two-body energy

spectrum [45,46]. Indeed, in 1D the energy spectrum of two interacting particles has a continuous set of scattering states and, for NN or on-site interaction, one bound state outside this region. If the interaction strength is strong enough the bound state is able to support the presence of localized solutions, like one-site bound pairs for on-site interaction [47] or intersite bound pairs for long-range interaction [48]. To be more specific about our model Eq. (2), for $V_i = 1$ two particles can lie in NN sites and once the interaction is suddenly brought to strong values, the systems is projected in a state with high energy. If such an energy corresponds to the one of a bound state, the system is not able to decay in the scattering region and remains trapped in an excited level. This is due to the fact that the system is isolated, i.e., the energy is conserved, and to the kinetic energy limitation induced by the lattice structure. As a consequence the two particles form a NN intersite bound pair which can tunnel with $J_{\text{eff}} \sim J^2/V$, namely much slower than the single-particle tunneling processes. In Fig. 4 two signals are visible meaning that the energy we are providing to the system is not sufficient to form all the possible bound pairs but only a fraction of particles are bounded while the rest behave as single ones, with a tunneling amplitude J. The fact that for strong enough V_f more than two signals contribute to the dynamics is because also three- and in general many-body bound states can be formed; see, for instance, Ref. [49] for the case with on-site interaction and [46] for NN interactions. Of course, the bigger the number of bounded particles, the slower the velocity associated with its expansion will be.

IV. ATTRACTIVE REGIME

For $-2 < V_i < 0$ the density distribution is still almost constant. This feature combined with the fact that the two-body energy spectrum for NN interacting particles is symmetric under the transformation $V \leftrightarrow -V$ makes it intuitive to understand that, in analogy with the LL-DW quench, the same multisignal propagation is observed for V_i in a LL regime and V_f in the deep PS one. On the contrary, the dynamics driven by quenching from a PS to a LL regime is completely unexplored and, as we will see, gives rise to a very different scenario with respect to the repulsive case. Due to strongly attractive NN interaction, all the N particles are compressed in $L/2$ lattice sites while the others are empty (see the first panel of Fig. 1). Due to the on-site infinite repulsion, the physical properties inside the occupied region are basically the same as of a classical system. Indeed, if we perform a global interaction quench fixing the position i of the connected density-density correlation function, Eq. (2), well inside this region we do not observe any signal propagation for a long time; namely the correlation function is fully classical until a characteristic time is passed. Actually, for $V < -2$ the GS is highly degenerate, meaning that the real GS density distribution of a PS state is uniform [50]. Consequently, if at $t = 0$ we break the degeneracy by applying small local chemical potentials and we let the system evolve without them the system will try to restore the GS degeneracy by letting the high-density region expand even if no interaction quenches are performed. Of course this case is different from the repulsive DW regime where the twofold GS degeneracy is broken by using an odd number of sites L. The crucial point is that the particles occupying the populated region need a certain time, which depends on the single-particle position, to expand. More precisely, once the evolution begins, the particle located at the border between the occupied and empty regions can tunnel in one empty site thus letting another NN particle tunnel, and

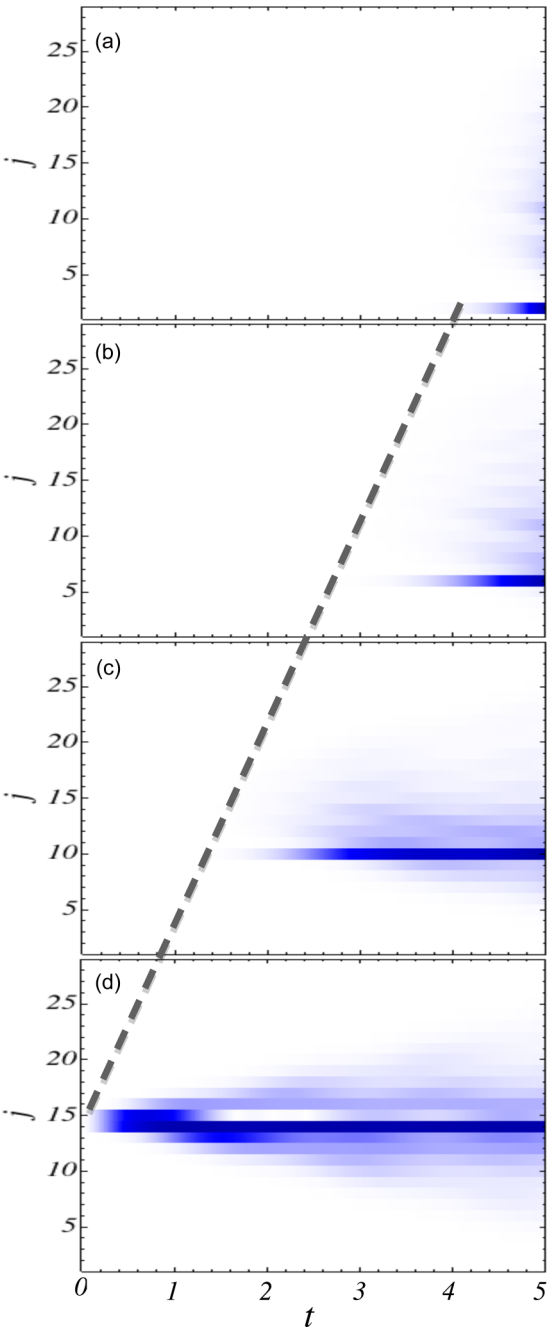

FIG. 5. t-DMRG results of $\Delta C_{ij} = |C_{ij}(t) - C_{ij}(0)|$ for $V_i = -4$ and $V_f = -1$ with (a) $i = 2$, (b) $i = 6$, (c) $i = 10$, (d) $i = 14$. The dashed line is given by Eq. (4). The chain length is $L = 30$ and $N = 15$. Both t and the V's are in units of J. The static simulations for the ground state are performed by keeping up to 512 DMRG states and 5 finite-size sweeps and using two antiparallel chemical potentials $\mu/J = 0.001$ in the lattice edges. In the dynamics the chemical potentials are removed and we use a time step $\delta = 0.01$ and 250 DMRG states.

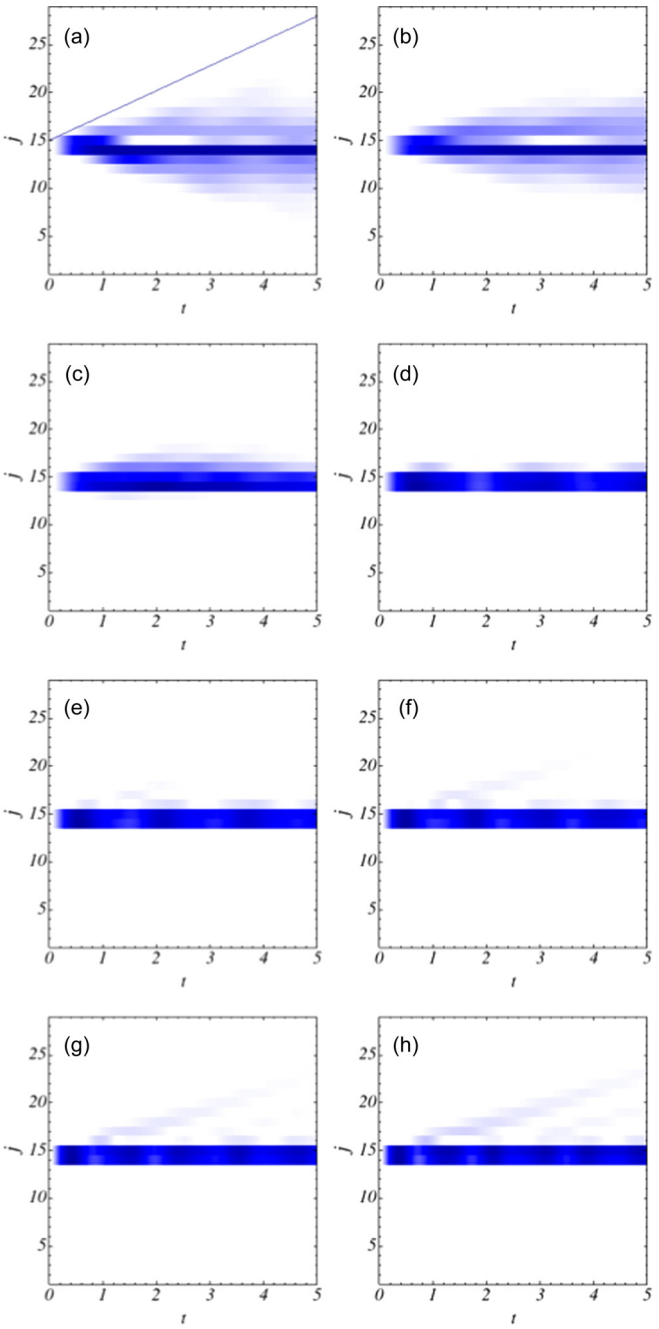

FIG. 6. t-DMRG results of $\Delta C_{ij} = |C_{ij}(t) - C_{ij}(0)|$ for $V_i = -4$ and (a) $V_f = -1$, (b) $V_f = -2$, (c) $V_f = -3$, (d) $V_f = -5$, (e) $V_f = -6$, (f) $V_f = -7$, (g) $V_f = -8$, (h) $V_f = -9$. The length of the chain is $L = 30$ and $N = 15$. Both t and the V's are in units of J. The slope of the solid lines in the first panel is the velocity v_{BA}, given by Eq. (3). The static simulations for the ground state are performed by keeping up to 512 DMRG states and 5 finite-size sweeps and using two antiparallel chemical potentials $\mu/J = 0.001$ in the lattice edges. In the dynamics the chemical potentials are removed and we use a time step $\delta = 0.01$ and 250 DMRG states.

so on. This kind of tunneling has a strong influence on the correlation spreading after an interaction quench. As a result what is very important for the dynamics is the position i in the connected density-density correlation function Eq. (2). Indeed, if one pins $i = 0$ one has to wait a long time before seeing any propagation signal due to the fact that all the other particles have to move first.

For the same reason, if i is pinned in a more central site the correlation propagation will appear sooner and clearly if i is located exactly at the border between the two regions with different densities the propagation will start immediately. These features are visible in Fig. 5 where we fixed i in different positions and the propagation starts at different times. As clearly shown in Fig. 5, for i pinned at different sites the propagation begins at different times. This behavior proves that once a sort of classic nature is imposed on an initial state, one has to wait a characteristic time before pure quantum effects, i.e., connected correlation spreading, take place. Calling i_0 the position of the border of the separated regions, from our numerical results we can estimate this waiting time

$$t \sim (i_0 - i)/3\,. \tag{4}$$

In the examples shown in Fig. 5, $i_0 = 15$ and $i = 2,6,10,14$, and the waiting times are given by Eq. (4). Finally in Fig. 6 we plot the propagation for $i = i_0$, namely at the border of the occupied and empty lattice regions for the GS. In this case, as discussed before, the time evolution of the quantum signals starts immediately. As shown in Fig. 6, starting from the PS phase, $V_i = -4$, and quenching in the LL we observe a quantum propagation spreading inwards and outwards in the region which was previously highly occupied at $t = 0$. The inner signal becomes weaker for $V_f < -2$ and almost disappears for $V_f < V_i$, namely quenching deep in the PS phase. In this regime, instead, there is still the outer propagation with a light-cone shape associated with ballistic transport and another even stronger signal localized at the center of the system. This latter effect is probably due to the formation of a many-body bound state which corresponds to a cluster of $\sim N$ particles. Clearly due to the large number of particles this cluster has an expansion velocity which is very small and it explains why for our time scale the signal remains mainly localized at the center of the lattice. From the other side, in analogy with the repulsive regime, the Bethe ansatz prediction, Eq. (3), is able to roughly capture the light-cone-like velocity propagation when the value of V_f is deep in the LL phase, while it fails approaching the phase transition. The Bethe ansatz velocity v_{BA}, indeed, goes to zero for $V_f \to -2$, while this is not the case for the velocity v of the correlation spreading, which is finite as shown in Fig. 6(b). Interestingly we get almost the same spreading velocity for any V_f in the gapped phase and its value $v \sim 2$ is much smaller than that observed for the repulsive case.

V. CONCLUSIONS

We studied the correlation spreading in an interacting integrable system after a sudden quench. We showed that depending on the initial condition, different excitation propagations can be observed. In particular, a quench from an initial density wave phase supports the presence of one clear light-cone signal. In this regime we found that the propagation velocity is, for a relatively large range of final interaction values, in good agreement with the Bethe ansatz predictions and then saturates to $v \sim 8$, for $V_f \gtrsim 5$. The situation is rather

different if the initial state is prepared in the Luttinger liquid phase. In this regime delocalized wave functions can give rise to a multisignal propagation for strongly interacting quenches. These different velocities are associated with the formation of bound states. Finally we studied the case when we start from a phase-separated state. Here, depending on the points where the connected correlation functions are measured, the propagation signals can be delayed. Moreover, for strong quenches, together with a weak signal of a ballistic evolution, with a spreading velocity $v \sim 2$ independent of V_f, also a very slow and strong signal associated with many-body bound states can be observed. As a last remark we stress that all our results can be proved in experiments involving either cold atoms or photons.

ACKNOWLEDGMENTS

We thank P. Calabrese for useful discussions. This work was supported by MIUR (FIRB 2012, Grant No. RBFR12NLNA_002). L.B. thanks the CNR-INO BEC Center in Trento for CPU time.

[1] A. Polkovnikov, K. Sengupta, A. Silva, and M. Vengalattore, Rev. Mod. Phys. **83**, 863 (2011).
[2] M. Rigol, V. Dunjko, and M. Olshanii, Nature (London) **452**, 854 (2008).
[3] J. M. Deutsch, Phys. Rev. A **43**, 2046 (1991).
[4] M. Rigol, V. Dunjko, V. Yurovsky, and M. Olshanii, Phys. Rev. Lett. **98**, 050405 (2007).
[5] A. Iucci and M. A. Cazalilla, Phys. Rev. A **80**, 063619 (2009).
[6] A. Coser, E. Tonni, and P. Calabrese, J. Stat. Mech.: Theory Exp. (2014) P12017.
[7] V. Alba and P. Calabrese, Proc. Natl. Acad. Sci. USA **114**, 7947 (2017).
[8] A. S. Buyskikh, M. Fagotti, J. Schachenmayer, F. Essler, and A. J. Daley, Phys. Rev. A **93**, 053620 (2016).
[9] R. Nandkishore and D. A. Huse, Annu. Rev. Condens. Matter Phys. **6**, 15 (2015).
[10] R. Vosk, D. A. Huse, and E. Altman, Phys. Rev. X **5**, 031032 (2015).
[11] G. De Chiara, S. Montangero, P. Calabrese, and R. Fazio, J. Stat. Mech.: Theory Exp. (2006) P03001.
[12] A. M. Läuchli and C. Kollath, J. Stat. Mech.: Theory Exp. (2008) P05018.
[13] S. R. Manmana, S.W essel, R. M. Noack, and A. Muramatsu, Phys. Rev. B **79**, 155104 (2009).
[14] G. Carleo, F. Becca, L. Sanchez-Palencia, S. Sorella, and M. Fabrizio, Phys. Rev. A **89**, 031602 (2014).
[15] L. Bonnes, F. H. L. Essler, and A. M. Läuchli, Phys. Rev. Lett. **113**, 187203 (2014).
[16] K. R. A. Hazzard, M. van den Worm, M. Foss-Feig, S. R. Manmana, E. G. Dalla Torre, T. Pfau, M. Kastner, and A. M. Rey, Phys. Rev. A **90**, 063622 (2014).
[17] P. Calabrese and J. Cardy, Phys. Rev. Lett. **96**, 136801 (2006).
[18] E. H. Lieb and D.W. Robinson, Commun. Math. Phys. **28**, 251 (1972).
[19] R. Sims and B. Nachtergaele, Lieb-Robinson bounds in quantum many-body physics, in *Entropy and the Quantum*, Vol. 529 of Contemporary Mathematics, edited by R. Sims and D. Ueltschi (American Mathematical Society, Providence, RI, 2010), pp. 141-176.
[20] M. Kliesch, C. Gogolin, and J. Eisert, Lieb-Robinson bounds and the simulation of time evolution of local observables in lattice systems, in *Many-Electron Approaches in Physics, Chemistry and Mathematics: A Multidisciplinary View*, edited by V. Bach (Springer, 2014), pp. 301-318.
[21] S. Bravyi, M. B. Hastings, and F. Verstraete, Phys. Rev. Lett. **97**, 050401 (2006).
[22] J. Eisert, and T. J. Osborne, Phys. Rev. Lett. **97**, 150404 (2006).
[23] M. Kastner, New J. Phys. **17**, 123024 (2015).
[24] P. Hauke and L. Tagliacozzo, Phys. Rev. Lett. **111**, 207202 (2013).
[25] J. Eisert, M. van den Worm, S. R. Manmana, and M. Kastner, Phys. Rev. Lett. **111**, 260401 (2013).
[26] L. Cevolani, G. Carleo, and L. Sanchez-Palencia, Phys. Rev. A **92**, 041603(R) (2015).
[27] L. Dell'Anna, O. Salberger, L. Barbiero, A. Trombettoni, and V. E. Korepin, Phys. Rev. B **94**, 155140 (2016).
[28] M. Kormos, M. Collura, G. Takács, and P. Calabrese, Nat. Phys. **13**, 246 (2016).
[29] I. Bloch, J. Dalibard, and W. Zwerger, Rev. Mod. Phys. **80**, 885 (2008).
[30] M. Cheneau, P. Barmettler, D. Poletti, H. Endres, P. Schau, T. Fukuhura, C. Gross, I. Bloch, C. Kollath, and S. Kuhr, Nature (London) **481**, 484 (2012).
[31] T. Langen, R. Geiger, M. Kuhnert, B. Rauer, and J. Schmiedmayer, Nat. Phys. **9**, 640 (2013).
[32] P. Jurcevic, B. P. Lanyon, P. Hauke, C. Hempel, P. Zoller, R. Blatt, and C. F. Roos, Nature (London) **511**, 202 (2014).
[33] P. Richerme, Z.-X. Gong, A. Lee, C. Senko, J. Smith, M. Moss-Feig, S. Michalakis, A. V. Gorshkov, and C. Monroe, Nature (London) **511**, 198 (2014).
[34] S. R. White and A. E. Feiguin, Phys. Rev. Lett. **93**, 076401 (2004); A. E. Feiguin and S. R. White, Phys. Rev. B **72**, 020404(R) (2005).
[35] L. Piroli, E. Vernier, and P. Calabrese, Phys. Rev. B **94**, 054313 (2016).
[36] See, e.g., T. Lahaye, C. Menotti, L. Santos, M. Lewenstein, and T. Pfau, Rep. Prog. Phys. **72**, 126401 (2009), and references therein.
[37] S. Baier, M. J. Mark, D. Petter, K. Aikawa, L. Chomaz, Zi Cai, M. Baranov, P. Zoller, and F. Ferlaino, Science **352**, 201 (2016).
[38] T. Fukuhara, P. Schau, M. Endres, S. Hild, M. Cheneau, I. Bloch, and C. Gross, Nature (London) **502**, 76 (2013).
[39] A. V. Gorshkov, J. Otterbach, E. Demler, M. Fleischhauer, and M. D. Lukin, Phys. Rev. Lett. **105**, 060502 (2010).
[40] R. J. Baxter, *Exactly Solved Models in Statistical Mechanics* (Academic Press, London, 1982).
[41] S. R. White, Phys. Rev. Lett. **69**, 2863 (1992).
[42] J. Friedel, Nuovo Cimento Suppl. **7**, 287 (1958).
[43] M. A. Cazalilla, R. Citro, T. Giamarchi, E. Orignac, and M. Rigol, Rev. Mod. Phys. **83**, 1405 (2011).
[44] M. Collura, P. Calabrese, and F. H. L. Essler, Phys. Rev. B **92**, 125131 (2015).
[45] J.-P. Nguenang and S. Flach, Phys. Rev. A **80**, 015601 (2009).

[46] M. Ganahl, E. Rabel, F. H. L. Essler, and H. G. Evertz, Phys. Rev. Lett. **108**, 077206 (2012).

[47] K. Winkler, G. Thalhammer, F. Lang, R. Grimm, J. Hecker Denschlag, A. J. Daley, A. Kantian, H. P. Buechler, and P. Zoller, Nature (London) **441**, 853 (2006).

[48] L. Barbiero, C. Menotti, A. Recati, and L. Santos, Phys. Rev. B **92**, 180406(R) (2015).

[49] M. Valiente, D. Petrosyan, and A. Saenz, Phys. Rev. A **81**, 011601(R) (2010).

[50] The density would be exactly constant in the presence of translational symmetry, i.e., in a ring geometry. In a boxlike geometry the density is almost constant in the center of the lattice showing oscillations at the edges.